Efficacy of analysis techniques in assessing broken wave loading on a cylinder upon a shoal

Dassanayake, Darshana T.; Raby, Alison; Antonini, Alessandro

DOI
10.1115/OMAE2019-96262

Publication date
2019

Document Version
Accepted author manuscript

Published in
Ocean Engineering

Citation (APA)
Dassanayake, D. T., Raby, A., & Antonini, A. (2019). Efficacy of analysis techniques in assessing broken wave loading on a cylinder upon a shoal. In *Ocean Engineering* (Vol. 7A-2019). Article OMAE 2019-96262 ASME. https://doi.org/10.1115/OMAE2019-96262

Physical Modelling of the Effect of Shoal Geometry on Wave Loading and Runup on a Cylinder

Darshana T. Dassanayake & Alison Raby
School of Engineering, University of Plymouth, UK

Alessandro Antonini
Faculty of Civil Engineering and Geosciences, Delft University of Technology, The Netherlands

Abstract: Estimation of impulsive wave loading and runup on a cylinder upon a shoal, typified by an offshore lighthouse on a partially emerged rock with a steep foreshore, poses a unique challenge to marine structural engineers. The foreshore geometry enables large waves to break at the base of the structure or in close proximity. The bore generated from the breaking wave has much higher velocities compared to oscillatory velocities in offshore conditions, and the highly aerated and turbulent nature of the flow makes it difficult to simulate using existing numerical models. Furthermore, most of the existing force models used to estimate impulsive forces acting on vertical cylinder are not directly applicable. Therefore, physical modelling investigations are the most feasible methods to study this phenomenon. This paper presents the data analysis techniques and the key findings of a series of small-scale wave flume tests conducted as a part of on-going research project: STORMLAMP – STructural behaviour Of Rock Mounted Lighthouses At the Mercy of imPulsive waves. This project is a collective effort of three UK universities: the University of Plymouth, the University of Exeter and University College London, which brings together expertise in both fluid and structural dynamics.

Keywords: Lighthouse, Impulsive wave force, Physical modelling, Wave loading

1 Introduction

Experimental investigations to determine impulsive wave loads and wave runup on offshore cylindrical structures has a history stretching back several decades. Several research studies on wave runup on vertical cylinders have been documented in the literature (Fig. 1). Those studies can be divided into analytical (e.g. Kim and Hue, 1989; Kriebel, 1990, 1992a; McCamy and Fuchs, 1954), experimental (e.g. De Vos et al., 2007; Hallermeier, 1976; Lykke Andersen et al., 2011; Martin et al., 2001; Niedzwecki and Duggal, 1992; Ramirez et al., 2013, Bonakdar et al. 2016, Cao et al. 2017) and numerical (e.g. Ramirez, 2012) studies. The current 'state of the art' numerical models generally produces accurate predictions of wave runup for typical offshore applications, but they are computationally expensive. Therefore, the semi empirical and analytical formulae are widely used for the estimation of the wave runup. These formulae (e.g. De Vos et al., 2007; Lykke Andersen et al., 2011) are based on maximum wave crest elevation (η_{max}) and horizontal particle velocity at the top of the wave crest (u). Therefore, in order to estimate the wave runup, estimation of wave kinematics using appropriate wave theories or numerical modelling is required. This paper focuses on wave runup and forces on a cylinder upon a shoal such as offshore rock lighthouses. The foreshore geometry of a shoal enables large waves to break at the base of the structure or in close proximity. This will make the wave kinematics at the base of the cylinder significantly different from previous scenarios and hence, available models will not be able to accurately predict the wave runup.

Similarly, seminal force models have been developed to estimate wave loading on cylinders using experimental data by Goda et al. (1966), Campbell and Weynberg (1980), Cointe and Armand (1987), Wienke and Oumeraci (2004), Burmester et al. (2017), Tu et al. (2018a and 2018b), Khansari and

Oumeraci (2018) and Khansari (2018). There is a significant difference between most of the previous studies on impulsive wave loads on offshore structures and the current study. In the current study as illustrated in Fig. 1, waves are not slamming into the cylinder with a near vertical face, rather waves are either breaking into the base of the cylinder or bores generated from broken waves are hitting the structure. The highly nonlinear phenomena make the study complex, with only a few experimental investigations having been carried out (e.g. Banfi, 2018). According to published bathymetric data (e.g. www.navionics.com) and recent bathymetric surveys carried out around prominent rock lighthouses in the UK, most of the rock shoals have slopes around 1:2 ~ 1:5 until they reach depths around 40m to 50m. (Trinity House, 2019a and 2019b). Therefore, the current research study considered steep slopes between 1:1 and 1:5.

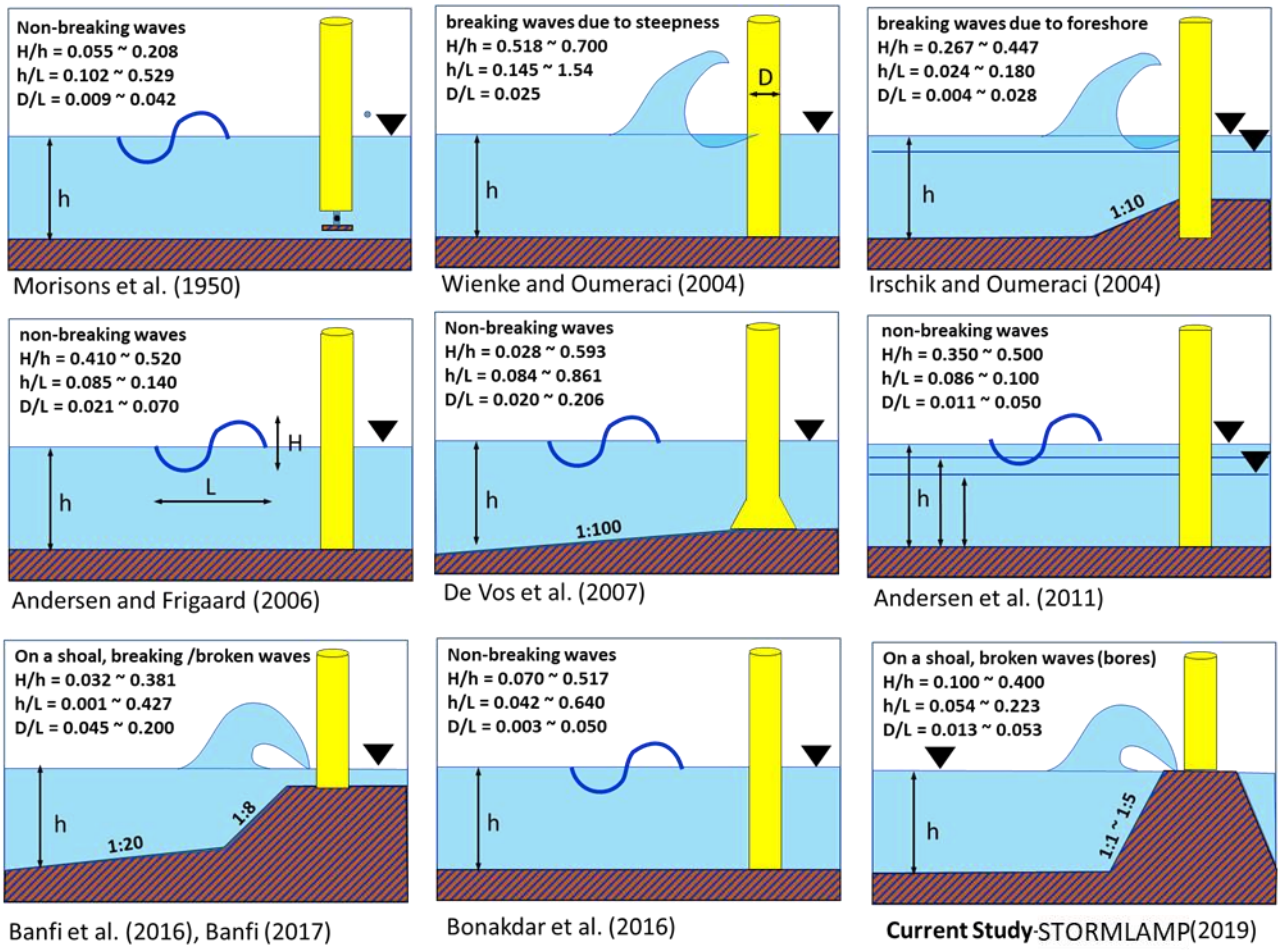

Fig 1: Comparative model setups of previous and current experimental investigations on wave forces and runup.

2 Physical Model Set-Up

The complicated foreshore bathymetry is simplified in the physical model to be a single slope, topped by a horizontal berm. The lighthouse is modelled as a vertical cylinder and incorporates several instruments. Model tests were performed in a wave flume (35 m long x 0.6 m wide x 1.2 m high) in the COAST Laboratory at the University of Plymouth (Fig. 2), using regular waves and focused wave groups. Regular wave tests enabled the simplest parametrization of conditions leading to wave breaking and the subsequent impact and wave runup on the cylinder, and are reported on here. The shoal width was 3Rc (where R_c = radius of the cylinder) and the cylinder was placed at the centre of the shoal. Three different foreshore slopes (1:1, 1:2.5 and 1:5) were used.

The water level corresponded with the top of the shoal, i.e. 0.5 m. The cylinder was suspended from the top of the flume, acting as a vertical cantilever, leaving a minimal gap between the bottom of the cylinder and horizontal top plate of the shoal, to ensure the cylinder was physically disconnected from the shoal but with no significant flow occurred beneath the cylinder. The top of the cylinder was

connected to a six-axis load cell. This setup enabled force measurement along three perpendicular axes, with three simultaneous torque measurements about those axes.

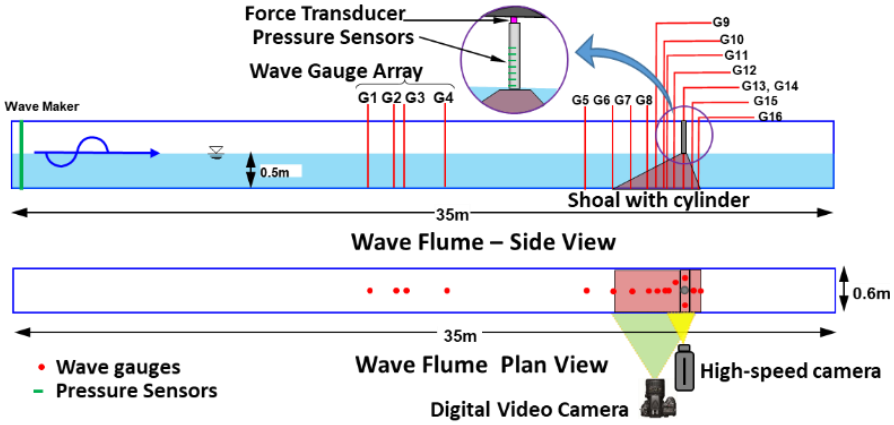

Fig 2: Experimental setup in 35m flume

A wave gauge array with 4 wave gauges was used for wave reflection analysis and a further 12 wave gauges measured water level around the model. The model setup consisted of a high-speed camera (125fps), a second digital video camera (50 fps), and a GoPro camera mounted near the top of the cylinder recorded each model tests (Fig 3). The high-speed and other digital video cameras were synchronised with the data acquisition system and those data were processed to obtain wave breaking location and wave runup along the cylinder.

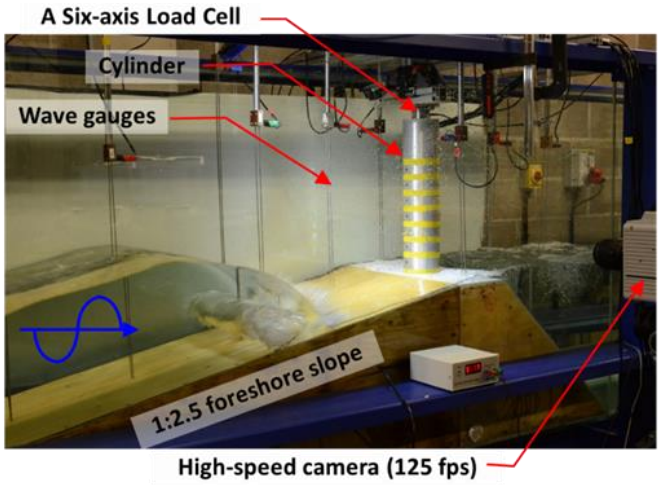

Fig. 3. Model setup for wave flume tests (left panel) and an exemplary force record (right panel)

Each model configuration was tested with a range of regular wave parameters as shown in Table 1. These parameters were carefully selected after analysis of probable extreme wave conditions occurring around exposed lighthouses such as Fastnet lighthouse (Antonini et al. 2019) and Wolf Rock lighthouse (Raby et al. 2019).

Tab. 1. Wave parameters

Model Scale [1:81]		Prototype Scale	
H [m]	T [s]	H [m]	T [s]
0.050	1.200	4.050	10.8
0.075	1.500	6.075	13.5
0.100	1.850	8.100	16.65
0.125	1.960	10.125	17.64
0.150	2.440	12.150	21.96
Cylinder diameter = 0.12m (9.72m in prototype scale)			

3 Data Acquisition and Analysis

The wave force acting on the cylinder has two force components: a rapidly-varying (impulsive/dynamic) component and a quasi-static component. When a test rig is exposed to a rapidly-varying wave forces, typically the dynamic responses of the test rig is measured, rather than the actual wave forces. The load cell with six-degrees of freedom hence measured the Total Force Responses (TFR) of the cylinder rather than the actual wave force. Therefore, careful data processing was required to separate force components from the measured signal. The TFR were analysed, firstly to separate the Total Force (TF) from recorded TRF signal and secondly to separate the impulsive and quasi-static force components of the extracted TF. The raw TFR signals were initially filtered in the frequency domain using a low-pass filter to remove high frequency electronic noises. The cut-off frequency of the low pass filter was set to 100Hz to make sure the cut-off limit was appropriately large compared to the useful frequencies in the measured TRF signal.

Prior to the wave tests, impact hammer tests were conducted to identify the natural frequency of the cylinder (the test rig). A calibrated PCB impulse force hammer (model 086C03) was used for these tests. The hammer was connected to the same data acquisition system and test data were recorded at a sampling frequency of 5 kHz. The frequency spectrum of the Total Force Response (TFR) signal recorded during the hammer tests were analysed and determined that the natural frequency of the cylinder was approximately 12 Hz).

A comparative study of the different data processing techniques in force measurements was performed using a wider data set and the Hilbert–Huang transform (HHT) technique was identified as the most suitable approach for the separation of the TF from TFR signals. The Hilbert–Huang transform (HHT) is an empirically based data-analysis method, which consists of two parts: Empirical Mode Decomposition (EMD) and Hilbert Spectral Analysis (HSA). TFR data acquired during the experiments are predominately nonlinear and they are generated by a nonstationary process. HHT is a proven technique to handle nonlinear nonstationary data. The Ensemble Empirical Mode Decomposition (EEMD) method (Wu and Huang, 2009), which is an improved technique based on HHT, was adopted for force separation. Once the TF was separated from the TFR, impulsive and quasi-static components were separated by the LOESS method (Locally Estimated Scatterplot Smoothing) e.g. Tu et al. (2018a and 2018b). A detailed description of the force analysis methodology followed during the current study and its validation were reported in Dassanayake et al. (2019).

3.1 Wave Runup Analysis

The high-speed camera captured wave impacts and wave runup along the cylinder at a rate of 125 fps. Each regular wave test consisted of 50 - 100 waves depending on wave period with a total test duration of 120s. However only the first 10 fully developed waves were captured using high-speed camera. The camera was synchronised with both the wave generation and data acquisition systems and to save hard disk space only 3,500 frames captured between time t = 20s and t = 50s of each test were saved (t = 0s is the start of the wave generation and data acquisition). A MATLAB code was developed to extract wave runup time series from these high-speed video records.

Fig 4 illustrates the key steps of wave runup measurement procedure. Fig 4a shows the field of view of the high-speed camera, and the calibration pattern used for the distortion correction and for scaling-up the images. The top surface of the horizontal berm was considered as the baseline for wave runup measurements. The water level was coincident with the top the shoal, i.e. 0.5m above the flume bed level. Fig 4b depicts wave runup. Both the high-speed images and the cylinder were grey scale, which limits the options for filtering the images. Hence, absolute difference between two images were used for detection of wave runup (Fig 4c); these absolute difference images provided wave runup corresponding to the second image. A mask was applied to each image to reduce the computational time while keeping only the interested area for further processing. The absolute difference image shown in Fig 4c was further filtered based on pixel thresholds, to obtain a cleaner image (Fig. 4d) to extract wave runup.

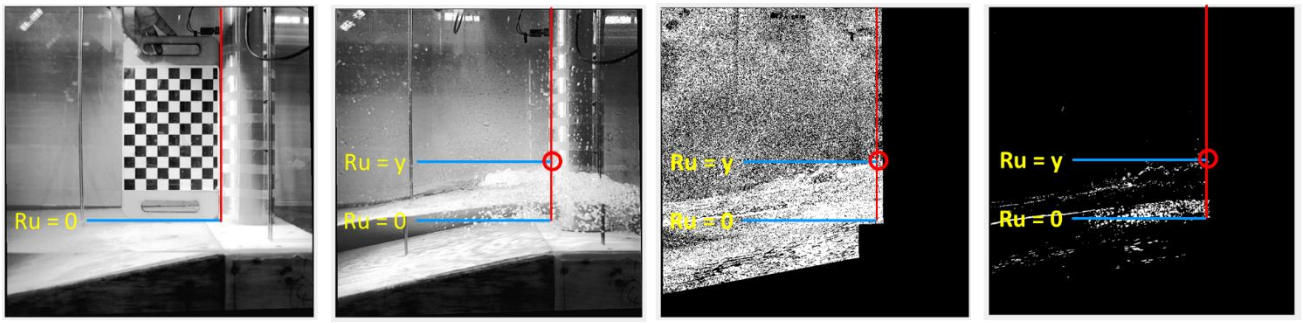

(a) Field of view and calibration pattern used for camera calibration

(b) Wave runup measurement along the reference line (red vertical line)

(c) Absolute difference of two consecutive images (After masking)

(d) Filtered Absolute difference image

Fig. 4. Wave runup calculation using high-speed camera images

The MATLAB code searches for the highest non-zero pixel in the filtered absolute difference images along the reference line (vertical red line in Fig. 4) and records the pixel coordinates against the frame number. These data are then converted to wave runup time series. Raw runup time series were filtered using the MATLAB Locally Estimated Scatterplot Smoothing (LOESE) function to remove any unwanted "spikes" in the time series. Fig. 6 depicts a typical wave runup time series extracted from the process. In order to verify the MATLAB procedure, peak runup values were manually identified from timestack images (Fig. 5). The timestack image consists of pixel values extracted along the reference line from each high-speed camera image. These pixel values were then sequentially arranged with the x-axis representing the frame number and the y-axis representing the runup height. The red continuous line marks the base of the cylinder. Peak runup values captured by the procedure were compared with the manually selected peaks as shown in Fig. 6.

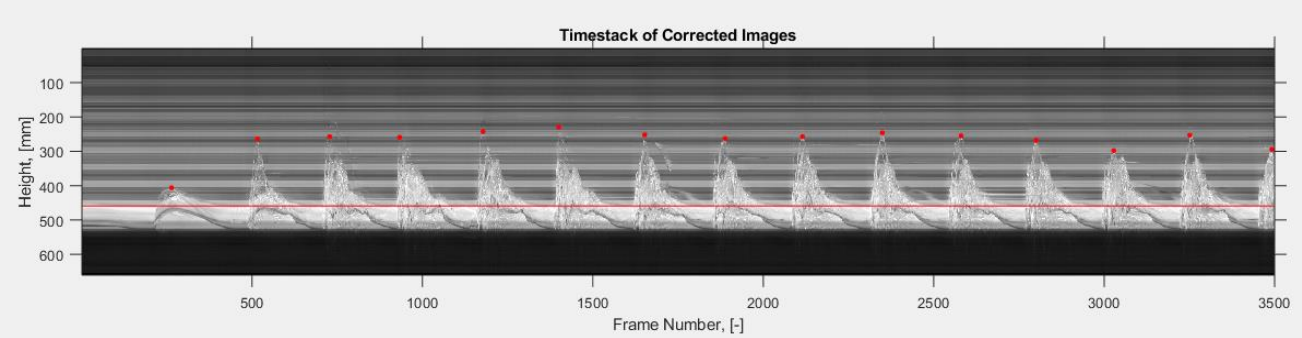

Fig. 5. A typical timestack of images recorded using the high-speed camera

The upper panel of Fig. 6 shows raw time series from the image analysis (green line) and filtered time series using LOESE. The figure also contains data from of wave gauge 13 and 14, which were aligned with the centre of cylinder, perpendicular to the wave direction and placed halfway between the cylinder and the glass walls of the flume (Fig. 2 and the upper panel of Fig. 6). Since the wave gauges were therefore one radius (Rc) of the cylinder behind the front face of the cylinder, there is a slight difference in the time where peaks are recorded. Nevertheless, water surface elevation from these two gauges were used for quality controlling of the wave runup analysis. Maximum wave runup for each wave within the selected time frame was extracted from the images. Even though the waves were generated as regular waves, note that there is a difference between each individual wave.

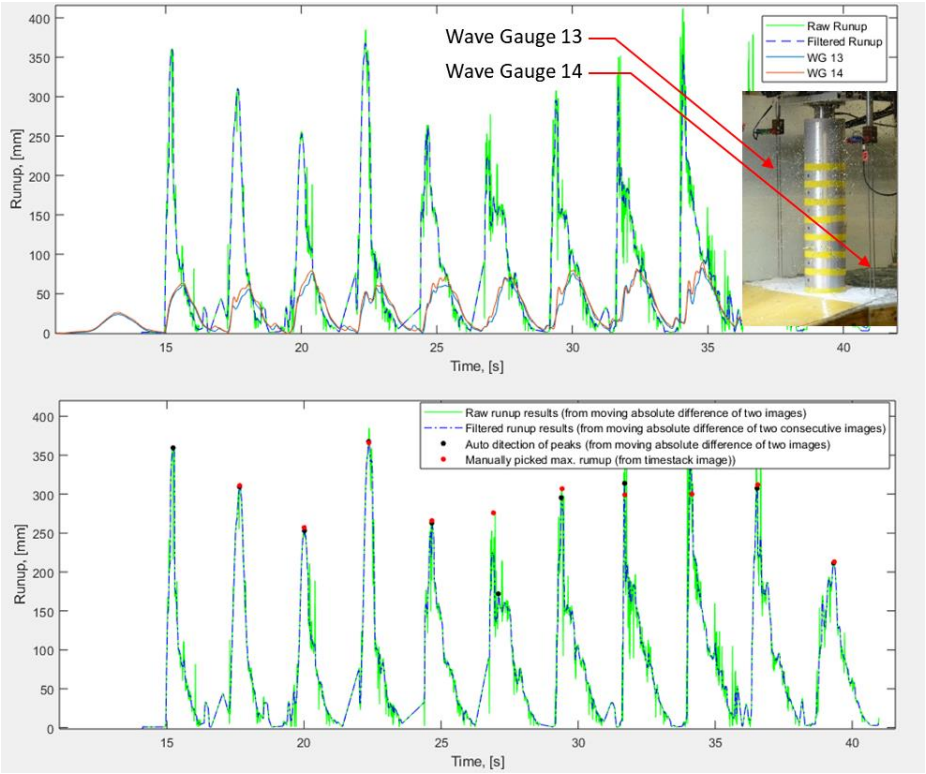

Fig. 6. A wave runup time series from image analysis and comparison of manually digitises and computer selected maximum runup

Approximately the first 10 fully developed waves were considered for each regular wave test. Individual wave runup measurements of those waves show fluctuations around ±10% of the mean wave runup. Therefore, mean values of the first 10 peak runup values corresponding to the first fully developed 10 waves were considered in the subsequent analysis. Fig. 7 compares the manually and computer selected mean runup values. Fig.7 shows good agreement for runup values up to 300mm beyond which the wave interactions usually resulted from violent wave breakings in front of the cylinder. This wave breaking will generate green water runup as well as spray. Often the MATLAB code was unable to pick the highest green water marks alone the reference line, instead, picking some spray just above. This limitation causes an overestimation of runup. Therefore, those peaks were manually digitised. Moreover, it is evident that agreement is less good as the slope becomes gentler. This behaviour is mainly related to the nature of the breaking wave generated on the gentler slope. On the 1:5 slope the waves break farther from the lighthouse than in the other cases, generating a very aerated bore where the colour of the flow is almost white, making it harder to be automatically detected.

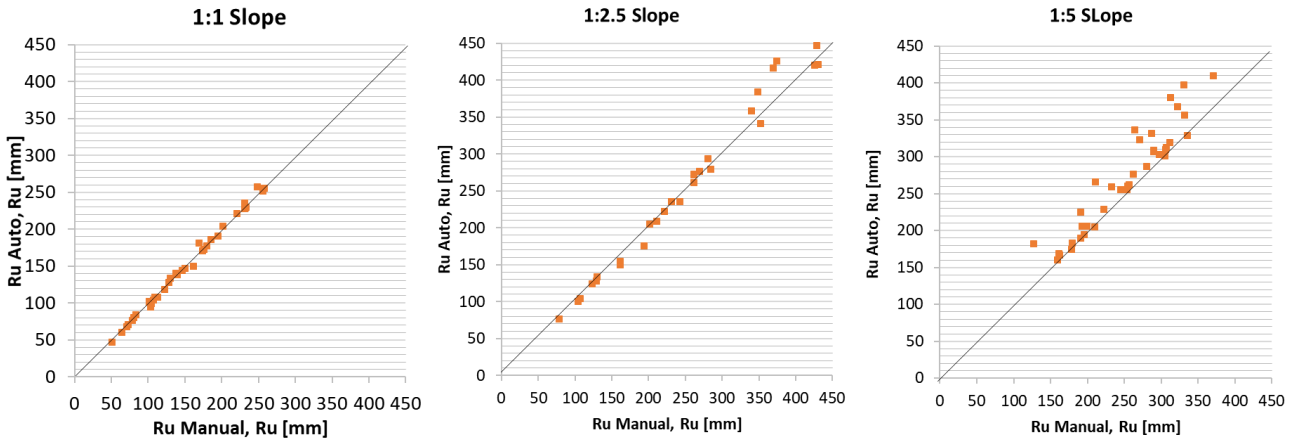

Fig. 7. Comparison of max. wave runup results from the MATLAB code and manually digitised values.

Fig. 8 illustrates the behaviour of wave runup measurements against wave period where solid black lines show the best fit to the data. In general, wave runup increases with wave height for all cases, with data points, particularly for smaller wave heights, showing a clear separation of best-fit lines. Incident wave height were obtained from wave reflection analysis performed at the wave gauge array located more than one wave length upstream from the toe of the shoal. The scatter towards the higher wave heights might result from wave runup measurement errors.

The steeper slopes (1:1 and 1:2.5) show a slight downward trend in wave runup measurement as the wave period increases. The larger wave tests with 1:2.5 slope resulted in the largest wave runup measurements for the entire test series. The 1:5 slope shows a light upward trend in wave runup measurements as illustrated in the right panel of Fig. 8.

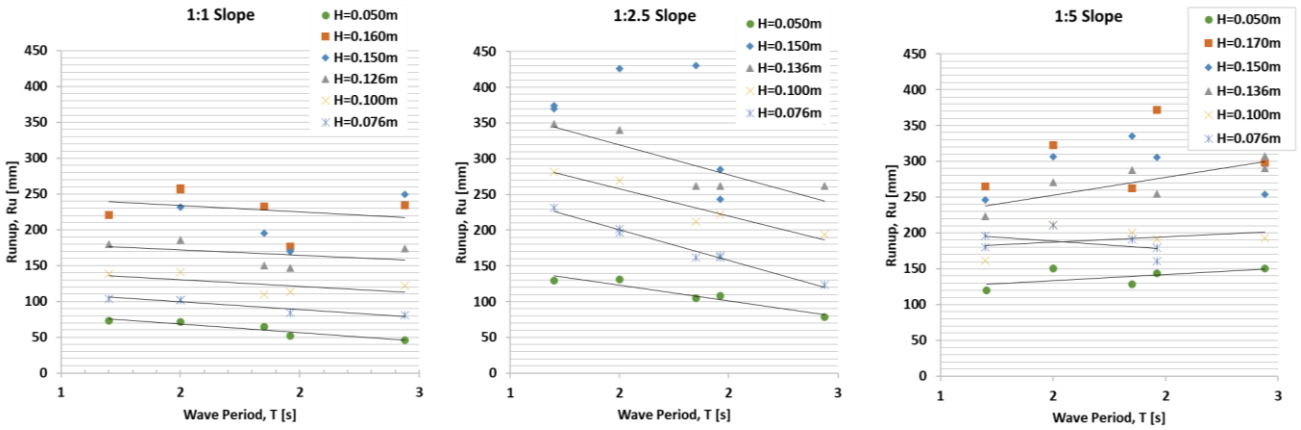

Fig. 8. Wave runup results for different slopes

Wave runup results from all three foreshore slopes were also plotted against offshore surf similarity parameter. Fig. 9 (left panel) shows the non-dimensional runup calculated by dividing the runup by the incident wave height. Fig 9 (right panel) shows the non-dimensional runup calculated by dividing wave runup by water depth. The right panel again indicates the large runup events recorded on the 1:2.5 slope. Note that the current study considered only a single water depth, hence d is a constant. Dotted lines in the figures shows the best-fit line of each data set.

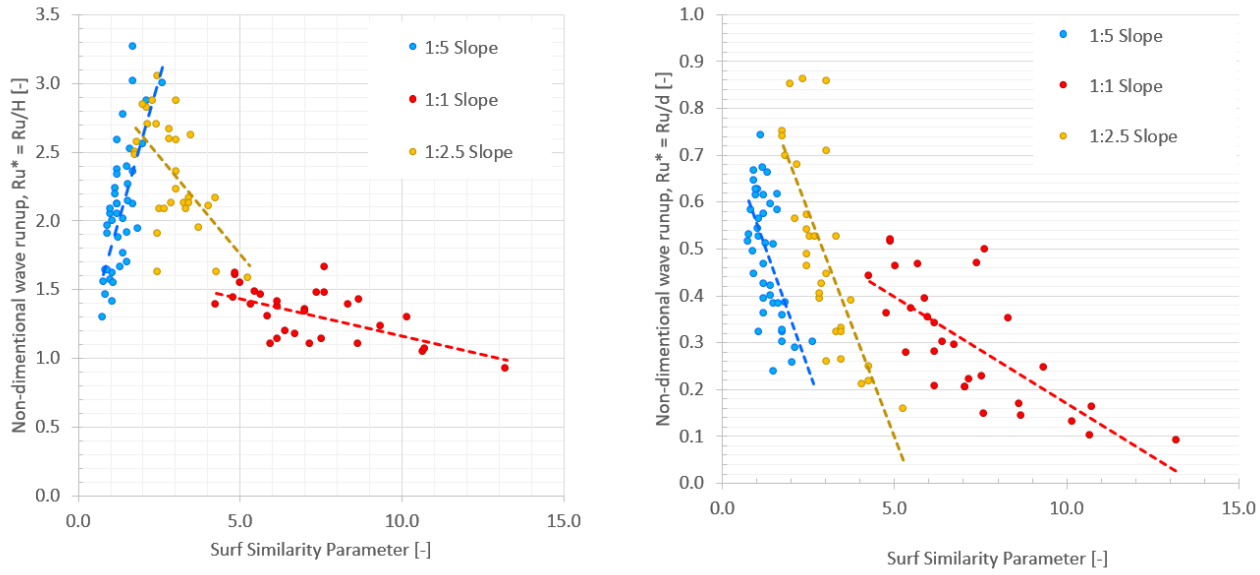

Fig. 9. Non-dimensional wave runup for all three slopes: runup divided by offshore incident wave heights (left) and runup divided by water depth at the toe of the shoal (right)

Both panels clearly illustrate that plunging breakers ($0.5 < \xi_0 < 3.3$) cause large runup events particularly for $1 < \xi_0 < 2$. In this range, wave runup could reach as much as 3 times the wave height. Wolf Rock lighthouse is on a rocky shoal with approximately 1:2.5 slope towards the main wave direction according to published bathymetric data. Therefore, findings of this physical modelling will help to understand the wave parameters that cause damage to the helideck in Bishop Rock, Longship and Wolf Rock lighthouses in the UK, which are more than 40m above the mean sea level.

3.2 Wave Load Analysis

A load cell with six-degrees of freedom measured the Total Force Responses (TFR) of the cylinder. The TFRs along the direction of wave propagation were extracted and processed to obtain Total Forces. A comparative study of empirical and physically based methods to extract TF from TFR were performed and Ensemble Empirical Mode Decomposition (EEMD) method (Wu and Huang, 2009, Huang et al., 2014) was selected as the most appropriate method to extract TFs as it is computationally less expensive compared to deconvolution technique without any loss of accuracy. A sensitivity analysis was performed to find optimum amplitude for white noise (which is defined as the ratio of the standard deviation of the added noise and that of pre-processed signal, Nstd) and "Ensemble number" (NE) for the EEMD. Nstd=0.06 and NE=100 were used for the current analysis. Measured raw Total Force Responses (TFR) signal was filtered using a 100Hz low pass filter to remove a large portion of electronic noise. This pre-processed signal was then further processed using the EEMD technique. Intrinsic Mode Functions (IMFs) 6 onwards were summed to generate the total Force (TF) signal. Total Force signals of each test were truncated to consider the first 10 fully developed regular waves. Then the mean value of these 10 peaks were used for further analysis described below.

Mean values of the maximum Total Forces were plotted against the surf similarity parameter as shown in Fig. 10. The Total Force increases as surf similarity parameter decrease, for the same wave period. Total Forces showed higher peaks when the surf similarity parameter is around 1 to 2, except 1:1 slope. Fig. 11 shows the non-dimensional Total Forces plotted against wave steepnesses (left panel) and surf similarity parameters (right panel). Higher non-dimensional Total Forces were recorded when wave steepness was higher, however, the large scatter of the data indicate a poor correlation between the Total Forces and the wave steepness. Generally, non-dimensional Total Forces were also higher when surf similarity parameter is between 1 and 5 indicating wave cases with potential plunging breakers cause maximum Total Forces at the cylinder as expected even in condition of broken wave loadings.

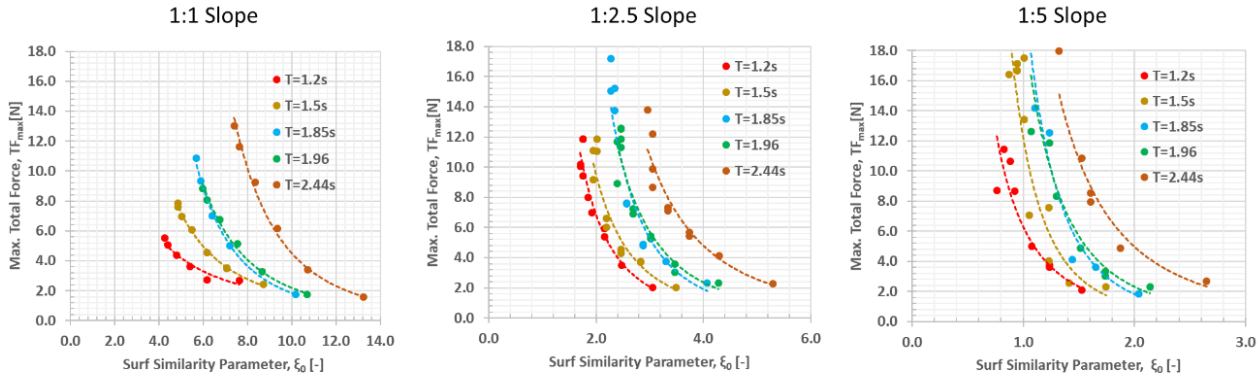

Fig. 10. Max. Total Forces for different shoal geometries

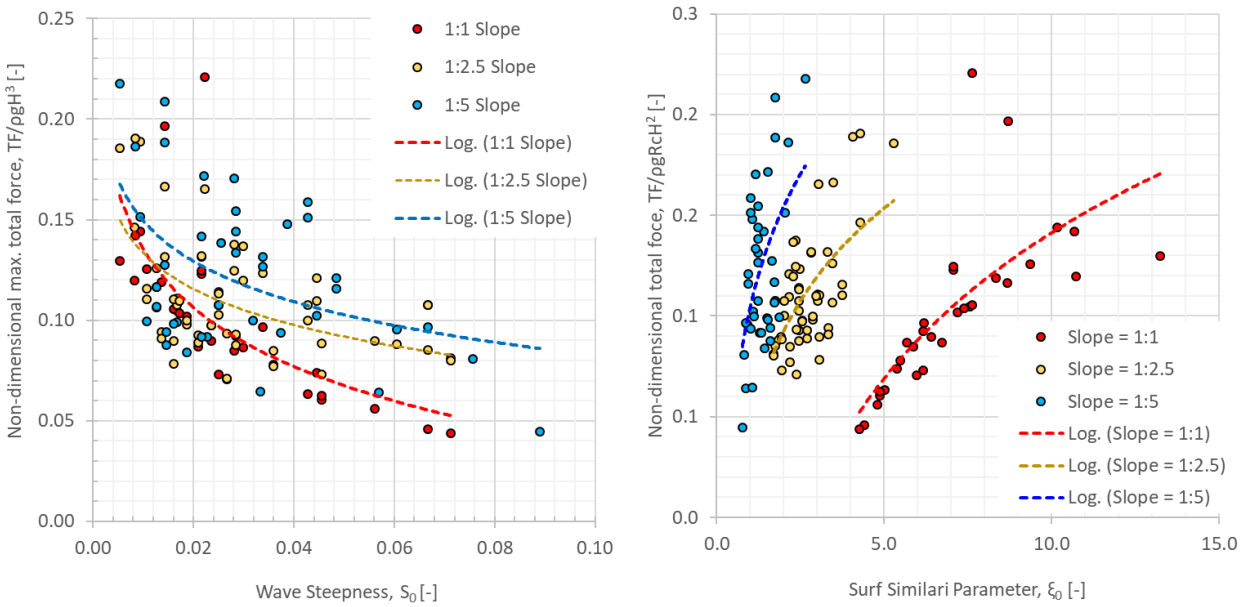

Fig. 11.Non-dimensional max non-dimensional total wave forces (TF_{max}*=$TF_{max}/\rho g R_c H^2$)

4 Concluding Remarks

This paper presents the key findings of an on-going research study on wave loading and runup on a cylinder upon a rocky shoal. The study mainly focuses on wave runup and Total Forces on a cylinder under the action of broken waves from regular wave tests. High-speed video records were analysed to obtain time series of wave runup on the front face of the cylinder. Total Force measurements and wave runup were further studied to understand the influences of wave parameters and steepness of foreshore slope.

New MATLAB code was developed to extract wave runup time series from high-speed video records. This code shows a good agreement with the manually digitised peaks, particularly for the low runup events. Therefore, the code will be used for the analysis of a wider data set. Furthermore, the code will assist in extracting wave runup alone several lines around the cylinder, which is essential for validation of CFD models.

As illustrated in this paper, both wave runup and Total Force increase as the surf similarity parameter decreases. This is mainly due to different breaker types and differences in residual energy in the bore generated from the wave breaking. In the case of a plunging breaker, as seen in most of the model tests discussed in this paper, impulsive loadings occur on the structure. The impact duration is much larger compared to slamming waves experienced by offshore structures in deeper water. This type of loading has a high potential to resonate cylindrical structures on rocky shoals such as lighthouses.

References

Antonini A., Raby A., Brownjohn J.M.W., Pappas A., D'Ayala D., 2019. Survivability assessment of Fastnet lighthouse. Coastal Engineering, Vol. 150: pp. 18-38, doi.org/10.1016/j.coastaleng.2019.03.007.

Banfi D., 2018. A field and laboratory study on the dynamic response of the Eddystone lighthouse to wave loading, PhD Thesis, University of Plymouth, UK.

Burmester S, de Ridder EJ, Wehmeyer C, Asp E, Gujer P., 2017. Comparing different approaches for calculating wave impacts on a monopile turbine foundation. ASME 2017 36th international conference on ocean, offshore and arctic engineering. American Society of Mechanical Engineers; 2017. V010T09A063, doi:10.1115/OMAE2017-61182.

Campbell I, Weynberg P., 1980. Measurement of parameters affecting slamming, Report No. 440, University of Southampton, Department of Aeronautics and Astronautics.

Cao D., Huang Z., He F. Jian W., Yat-Man E.L., 2017. An improved prediction for wave runup on a circular cylinder,. Coastal Engineering Journal, 2017, Vol. 59 (3: 1750013), doi.org/10.1142/S0578563417500139.

Cleveland WS., 1979. Robust locally weighted regression and smoothing scatterplots. Journal of the American Statistical Association 1979; Vol. 74(368): pp. 829-836.

Cointe R., Armand J.L., 1987. Hydrodynamic impact analysis of a cylinder. Journal of Offshore Mechanics and Arctic Engineering, 1987; Vol. 109(3): pp. 237–43, doi:10.1115/1.3257015.

Dssanayake D.T., Raby A.C., Antonini A., 2019. Efficacy Of Analysis Techniques In Assessing Broken Wave Loading On A Cylinder Upon A Shoal, Proceedings of the ASME 2019 38th International Conference on Ocean, Offshore and Arctic Engineering OMAE2019, Glasgow, Scotland.

De Vos, L., Frigaard, P., De Rouck, J., 2007. Wave run-up on cylindrical and cone shaped foundations for offshore wind turbines. Coastal Engineering, Vol. 54(1), pp. 17–29, doi.org/10.1016/j.coastaleng.2006.08.004.

Goda Y, Haranaka S, Kitahata M. 1966. Study of impulsive breaking wave forces on piles, Report of Port and Harbour Technical Research Institute. 5., 1966. pp. 1–30. (6) (Original report in Japanese).

Hallermeier, R.J., 1976. Nonlinear flow of wave crests past a thin pile, Journal of the Waterways, Harbors and Coastal Engineering Division, 1976, Vol. 102 (4), pp. 365–377.

Huang, N.E., Shen, Z., Long, S.R., Wu, M.C., Shih, H.H., Zheng, Q., Yen, N., Tung, C.C. and Liu, H. H., 1998. The empirical mode decomposition and the Hilbert spectrum for nonlinear and non-stationary time series analysis, 454, Proceedings of the Royal Society of London. Series A: Mathematical, Physical and Engineering Sciences, http://doi.org/10.1098/rspa.1998.0193

Huang, N.E., Shen, S.S.P. Editors, 2014. Hilbert–Huang Transform and Its Applications, Second Edition, Interdisciplinary Mathematical Sciences: Vol. 5, ISBN 978-981-4508-23-0, World Scientific Publishing Co. Pte. Ltd.

Irschik K, Sparboom U, Oumeraci H., 2004. Breaking wave loads on a slender pile in shallow water. Proceedings 29th International Conference on Coastal Engineering (ICCE), ASCE, Vol. 1, Lisbon, Portugal, World Scientific, 2005; pp. 568-580.

Khansari, A., 2017. Dynamic Response of Jacket Structures to Breaking and Non-breaking Waves, PhD Thesis, Technischen Universität Braunschweig, Germany, 10.24355/dbbs.084-201808091032-0.

Khansari, A. Oumeraci, H., 2017. Impact forces due to breaking waves on jacket structures for offshore wind turbines (in German), 20th "JuWi-Treffen", Darmstadt, Germany.

Kim, M.H., Hue, D.K.P., 1989. The complete second-order diffraction solution for an axisymmetric body part 1. monochromatic incident waves, Journal of Fluid Mechanics. Vol. 200, pp. 235–264, doi.org/10.1017/S0022112089000649.

Kriebel, D.L., 1990. Nonlinear wave diffraction by vertical circular cylinder. Part I: diffraction theory. Ocean Engineering, Vol. 17, pp. 345–377, doi.org/10.1016/0029-8018(90)90029-6.

Kriebel, D.L., 1992a. Nonlinear wave interaction with a vertical cylinder. Part II: wave runup. Ocean Engineering, Vol. 19 (1), pp. 75–99, doi.org/10.1016/0029-8018(92)90048-9.

Kriebel, D.L., 1992b. Nonlinear wave runup on large circular cylinders. Proceedings Civil Engineering in the Oceans V, ASCE, pp. 173–187.

Lykke Andersen, T., Frigaard, P., 2006. Horns Rev II, 2-D model tests. Wave run-up on pile,.DCE Contract Report No. 3. Aalborg University, Denmark.

Lykke Andersen, T., Brorsen, M., 2007. Horns Rev II, 2-D model tests: Impact pressures on horizontal and cone platforms from irregular waves, DCE Contract Report No. 13, Aalborg University, Denmark.

Lykke Andersen, T., Frigaard, P., Damsgaard, M., De Vos, L., 2011.Wave run-up on slender piles in design conditions-model tests and design rules for offshore wind. Coastal Enginering, Vol.58, pp. 281–289.

Martin, A.J., Easson,W.J., Bruce, T., 2001. Run-up on columns in steep, deep water regular waves. Journal of Waterway, Port, Coastal, and Ocean Engineering, Vol. 127 (1), pp. 26–32, doi.org/10.1061/(ASCE)0733-950X(2001)127:1(26).

McCamy, R., Fuchs, R., 1954. Wave forces on piles: A diffraction theory, Technical Memorandum 69. U.S. Beach Erosion Board, U.S. Army Corps of Engineers.

Raby A.C., Antonini A., Pappas A., Dssanayake D.T., BrownjohnJ., D'Ayala D., 2019. Wolf Rock lighthouse: past developments and future survivability under wave loading, Proceedings of the Royal Society of London. Series A: Mathematical, Physical and Engineering Sciences.

Ramirez, J., 2012.Wave Run-Up on Offshore Wind Turbines: Numerical and Experimental Results. (Ph.D. thesis). Department of Civil Engineering, Alborg University.

Ramirez, J., Frigaard, P., Lykke Andersen, T., De Vos, L., 2013. Large scale model test investigation on wave run-up in irregular waves at slender piles. Coastal Engineering, Vol. 72, pp. 69–79, doi.org/10.1016/j.coastaleng.2012.09.004

Trinh, Q., Raby, A., Banfi, D., Corrado, M., Chiaia, B., Rafiq, Y., Cali, F., 2016. Modelling the Eddystone Lighthouse response to wave loading. Engineering Structures, 125, 566-578, doi.org/10.1016/j.engstruct.2016.06.027.

Trinity House, 2019a. Single Beam Echo Sounder Survey of Bishop Rock Lighthouse.

Trinity House, 2019b. Single Beam Echo Sounder Survey of Wolf Rock Lighthouse,

Tu, Y., 2018. Wave Slamming Forces on Offshore Wind Turbine Jacket Substructures, PhD Thesis (ISBN 978-82-326-3265-7), Norwegian University of Science and Technology, Norway.

Tu, Y., Cheng, Z., Muskulus, M., 2018a. Global slamming forces on jacket structures for offshore wind applications, Marine Structures, 58 (2018), pp. 53-72, doi.org/10.1016/j.marstruc.2017.11.001.

Tu, Y., Cheng, Z., Muskulus, M., 2018b. A global slamming force model for offshore wind jacket structures, Marine Structures, Vol. 60, July 2018, pp. 201-217, doi.org/10.1016/j.marstruc.2018.03.009.

Wienke, J., Oumeraci, H., 2005. Breaking wave impact force on a vertical and inclined slender pile-theoretical and large-scale model investigations. Coastal Engineering, Vol. 52, pp. 435-462

Wu, Z., Huang, N. E., 2004. A study of the characteristics of white noise using the empirical mode decomposition Proceedings of the Royal Society of London. Series A: Mathematical, Physical and Engineering Sciences, 460, pp. 1597–1611, doi.org/10.1098/rspa.2003.1221

Wu, Z., Huang, N. E., 2009. Ensemble Empirical Mode Decomposition: a noise-assisted data analysis method, Advances in Adaptive Data Analysis, Vol.1, No.1. pp. 1-41, doi.org/10.1142/S1793536909000047